Biointerface Research in Applied Chemistry
Open-Access Journal (ISSN: 2069-5837)

Article
Volume 13, Issue 6, 2023, 585
https://doi.org/10.33263/BRIAC136.585

Physicochemical Characterization of an Irbesartan Inclusion Complexes with Modified β-Cyclodextrins Prepared by Optimizing Process Variables and Employing Microwave Irradiation Technique

Venkata Ramana Maddula [1,2], Rama Sekhara Reddy Dachuru [3,*]

[1] Department of Pharmaceutical Sciences, Vignan's Foundation for Science, Technology & Research, Vadlamudi; mvramanapharmacist@gmail.com (V.R.M.);
[2] Faculty of Pharmacy, Krishna University, Machilipatnam-521004, Andhra Pradesh
[3] Department of Chemistry, Krishna University, Machilipatnam, Andhra Pradesh, 521004 India; dachuru@gmail.com (R.S.R.D.);
* Correspondence: mvramanapharmacist@gmail.com; dachuru@gmail.com (R.S.R.D.);

Scopus Author ID 13103061600
Received: 19.01.2023; Accepted: 21.02.2023; Published: 7.04.2023

Abstract: The purpose of the study is to investigate the influence of modified β-cyclodextrins like sulfobutyl ether β-cyclodextrin (SBE7-β-CD) and methyl-β-cyclodextrin (Me-β-CD) on the dissolution of irbesartan. Phase solubility investigations showed AL-type curves for modified β-cyclodextrins. The estimated apparent stability constant for irbesartan SBE7-β-CD is 716 ± 0.69 M^{-1}, whereas for irbesartan Me-β-CD is 584 ± 0.5 M^{-1}. The inclusion complexes of irbesartan SBE7-β-CD and irbesartan Me-β-CD in the equal molar ratio were prepared by microwave irradiation. The process parameters were optimized with 32 factorial designs. Response surface graphs and contour plots showed how process factors affected drug content. The inclusion complexes prepared by optimizing process variables are characterized. The dissolution rate of the prepared SBE7-β-CD complex with microwave irradiation technique showed 6.31 folds, and the Me-β-CD complex showed 6.04 folds improved dissolution rate compared to pure irbesartan. The studies conclude that prepared inclusion complexes are promising for increasing irbesartan bioavailability.

Keywords: irbesartan; inclusion complexes; sulfobutyl ether β-cyclodextrin (SBE_7-β-CD); methyl-β-cyclodextrin (Me-β-CD); microwave irradiation; bioavailability.

1. Introduction

Irbesartan is a subtype AT1 antagonist for the angiotensin II receptor. Its scientific name is 2-Butyl-3-[[4-[2-(2H-tetrazol-5-yl) phenyl] phenyl] methyl]-1,3-diazaspiro [4, 4] non-1-en-4-one shown in Figure 1. It is part of the system comprising renin, angiotensin, and aldosterone and belongs to a group of drugs called angiotensin receptor blockers [1,2]. The Biopharmaceutical Classification System (BCS) categorizes irbesartan as a molecule of class II, which is water-insoluble and highly permeable. Due to its limited water solubility, irbesartan has a low bioavailability [3,4]. The oral bioavailability reported is 60% [5]. Although several approaches for improving water-insoluble drugs' physicochemical and biological characteristics have been developed, each has limitations [6,7]. Numerous strategies have been proposed in order to solve this issue. One of the more promising methods among them is the

complexation of the drug with cyclodextrins. Oligosaccharides with varying glucopyranose rings are cyclodextrins. Lipophilic core and hydrophilic shell best describe cyclodextrins, which makes them appropriate for lipophilic drug inclusion complexes with lipophilic drugs. The complexation of drugs with cyclodextrins using a variety of methodologies indicated the value of cyclodextrins in enhancing the solubility qualities of pharmaceuticals [8-13]. Complexing with β-cyclodextrin and 2-hydroxypropyl β-cyclodextrin enhances Irbesartan solubility and dissolution, according to the literature [14,15]. However, toxicological concerns hinder the use of cyclodextrins in medications. With the exploration of numerous chemically altered cyclodextrins, such as methyl-β-cyclodextrin (Me-β-CD) and sulfobutyl ether β-cyclodextrin (SBE7-β-CD), represented in Figure 1, that have significantly lower toxicity, interest in the use of cyclodextrins has increased, especially for increasing dissolution, stability, and bioavailability of drugs that are low water soluble [16-19]. Sulfobutyl ether β-cyclodextrin (SBE7-β-CD) is a type of β-CD that has been modified chemically that is a negatively charged cyclic hydrophilic oligosaccharide in aqueous media. At 25 °C, aqueous solubility is 70 g/100 ml, much greater than β-CD.

Furthermore, unlike β-CD, there is no nephrotoxicity [20]. Methyl-β-cyclodextrin (Me-β-CD) has a considerable advantage over β-CD as a host molecule since it is more soluble than β-CD, i.e., 100 mg/ml and 0.18 g/ml, respectively [21]. It is thought that the higher solubility of (Me-β-CD) in water will help the drug dissolve effectively when it is complex [22,23]. Due to these benefits, SBE7-β-CD and Me-β-CD may improve the physiochemical properties of weakly water-soluble compounds. Inclusion complexes are traditionally prepared using a variety of methods. Co-evaporation, spray drying, and freeze drying are examples of these techniques. All these procedures have two key drawbacks: they are time-consuming and require substantial amounts of organic solvent. To avoid the drawbacks of existing complexation procedures, a novel technology such as microwave irradiation (MWI) is being explored. On the other hand, MWI will have fewer scale-up issues [24-27]. The study aims to synthesize inclusion compounds with optimized process parameters and determine the effect of modified cyclodextrins on irbesartan dissolution.

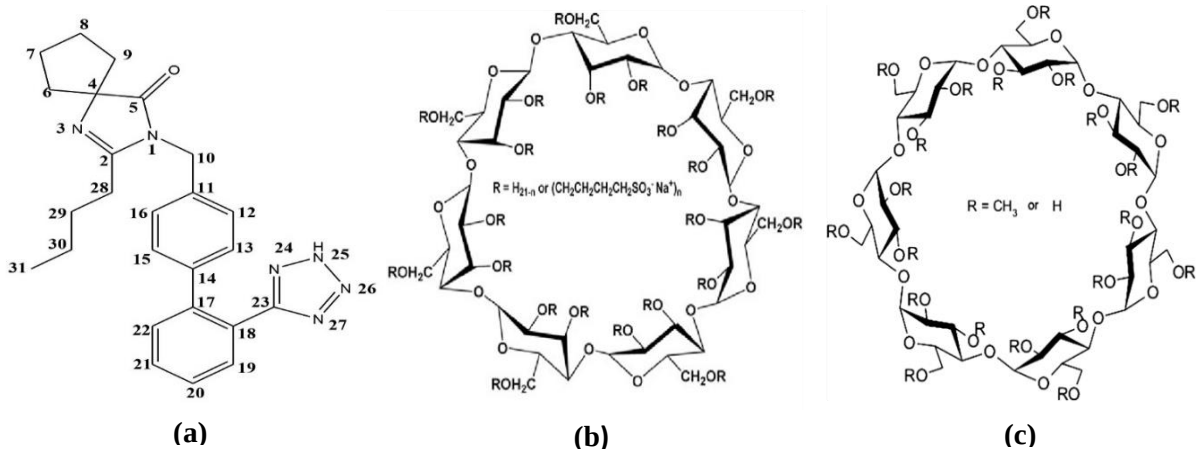

(a) (b) (c)

Figure 1. (a) Structure of Irbesartan; **(b)** Sulfobutyl ether β-cyclodextrin **(c)** Methyl-β-cyclodextrin.

2. Materials and Methods

2.1. Materials.

Irbesartan is obtained as a gift sample from Aurobindo Pharma Limited, Hyderabad. SBE7-β-CD is acquired from Shanghai-based Chembest Research Laboratories Limited, and

Methyl-β-cyclodextrin is purchased from BLD Pharmtech Pvt Ltd., Hyderabad. Every other substance, including solvents, was of analytical grade.

2.2. Analysis of drug content.

An inclusion complex containing 150 mg of irbesartan was dissolved and filtered through a membrane filter in ethanol. A UV-visible spectrophotometer at 244 nm was used to determine the amount of irbesartan in the filtrate [28].

2.3. Phase solubility studies.

Regarding irbesartan and cyclodextrin stoichiometry, phase solubility studies are performed. Phase solubility measurements of cyclodextrins and irbesartan were performed using the Higuchi-Connors technique [29]. An excess of irbesartan was added to 10 ml of distilled water containing various increased concentrations of Me-β-CD or SBE7-β-CD separately in different stoppered conical flasks. The suspension was shaken for 24 hours and then filtered via 0.45 μm filter paper, diluted as needed, and analyzed. According to the following equation, we were able to deduce the constant stability Ks using the phase-solubility diagram.

$$Ks = \frac{slope}{So(1 - slope)}$$

where S0 is the irbesartan water solubility.

2.4. Preparation inclusion complexes.

2.4.1. Preparation of Physical mixtures.

The preliminary phase solubility investigations produced an equal molar ratio (1:1) mixture of irbesartan and cyclodextrins. The physical mixture (PM) was made by combining correctly weighed quantities in a mortar for two minutes with a spatula [30].

2.4.2. Kneading method.

To prepare the equal molar binary system via the kneading technique, weighed amounts of irbesartan and cyclodextrins were placed in a mortar and mixed for 20 minutes. The final mixture was kneaded for a further 45 minutes with a few drops of ethanol. The resultant paste was dried overnight in a vacuum desiccator. The dried product was collected after passing through screen number 60 [31].

2.4.3. Microwave irradiation technique.

2.4.3.1. Preliminary trials.

In order to make inclusion compounds, it is crucial to understand the process variables. A mixture of irbesartan and either modified cyclodextrin in a 1:1 molar ratio with a small quantity of ethanol was subjected to microwave treatment in a microwave oven with a single magnetron emitter operating at 2.45 GHz. On the instrument's Pyrex turntable, the sample was rotated to achieve consistent irradiation. The solvent quantity is kept constant in both conditions. The irradiated samples were stored in a desiccator [32-34].

2.4.3.2. Optimization of process variables:

Preliminary trials were undertaken to establish the processing range of independent variables. The effect of processing parameters, i.e., power and reaction time, was examined using an experimental design and statistical data analysis [35]. The process parameters were optimized using a 3^2-factorial design. Three independent variables were chosen, namely microwave power 400 W to 900 W (X_1), reaction time 10 seconds to 240 seconds (X_2), and percentage drug content (R) as a dependent variable. Each independent variable consisted of three levels, which were represented by the values -1, 0, and +1, respectively. The quadratic model proved statistically significant at $p<0.05$ in the process optimization data analysis. Stat-Ease Design Expert 12 developed quadratic terms for the response variable in polynomial models utilizing multiple linear regression analysis. The following polynomial equation gives a description of the influence that independent factors have on variables that are dependent on them [36]:

$$R = \alpha_0 + \alpha_1 X_1 + \alpha_2 X_2 + \alpha_{12} X_1 X_2 + \alpha_{11} X_1^2 + \alpha_{22} X_{22}^2$$

In the above equation, R represents the dependent variable. The value α_0 represents the intercept as well as the mean of nine runs. The values α_1, α_2, α_{12}, α_{11}, and α_{22} represent the estimated variable coefficients X_1, X_2, X_1X_2, X_{12}, and X_{22}, respectively. The main effect of X_1 and X_2 is the average consequence of changing one variable from low to high. When two factors are changed simultaneously, the interaction terms X_1X_2 show how the parentage drug content varies. If the predicted and adjusted R^2 was within 0.20, the data or model might be incorrect. The coefficient was significant if $p < 0.05$. SNR determines precision. It compares the design point prediction range to the typical forecast error. Ratios over four suggest adequate model discrimination. The significance of the model was assessed using a one-way analysis of variance ($p < 0.05$) [37].

2.4.3.3. Verification of optimization capability.

Numerical optimization is desirability-based, and graphical optimization with the use of overlay graphs was used to review the developed mathematical model's optimization potential in light of the 32-factorial design findings. An optimal process was developed by imposing constraints on the minimum and maximum values for each factor and response. The factors' optimal ranges were constrained to $400 \leq X1 \leq 900$ W and $10 \leq X2 \leq 240$ sec; while response ranges were limited to: $85 \leq Y1 \leq 98$ %. Estimated model accuracy is obtained by preparing inclusion complexes with three sets of conditions having the optimal combination of the factors recommended by the program. The chosen optimized process variables were employed to prepare the inclusion complex to get a target value of 95 percent drug content. The relative percentage error was calculated by [37]:

$$\%\ Error = \frac{\text{Experimental value} - \text{Predicted value}}{\text{Predicted value}} \text{ X } 100$$

2.5. Studies on in vitro dissolution rate.

The dissolution rate of irbesartan and irbesartan inclusion systems was performed under sink conditions in 1000ml of 0.1 N hydrochloric acid. The dissolution studies were conducted employing a dissolving rate test device of type 2 USP XXIII. In the test, a paddle speed of 50

rpm was employed for 20 minutes at a temperature of 37±0.5 °C. An amount containing 150 mg equivalent to irbesartan was placed in each basket. A 0.45 µm nylon disc filter was used to filter a five ml aliquot taken at various times. If needed, the samples were diluted and analyzed spectrophotometrically at 244 nm [38].

2.6. Fourier transform infrared spectroscopy.

The FTIR spectra were taken using a CARY 630 from Agilent Technologies in the USA Spectrophotometer using the KBr pellet method. The scans were taken at a scanning speed of 2 mm per second with a resolution of 4 cm^{-1}, scanning the range between 600–4000 cm^{-1} while the device was operating dry purge [39].

2.7. Thermal analysis.

Differential scanning calorimetry (DSC) analysis was performed by Exstar 7020, Hitachi HTG, Japan, utilizing a 5 mg sample at 10 °C per minute from 40 to 300 °C. The reference was an empty aluminum pan. All studies employed 30 ml per minute of nitrogen gas [40].

2.8. Powder X-ray diffraction.

A Rigaku Miniflex 600 X-ray diffractometer was used to examine the crystalline state of irbesartan in prepared inclusion complexes. Cu Kα radiation at 40kV and 15mA was used as the X-ray source. Continuous mode scan at 5° per minute, scanning range 0–90 °[41].

2.9. Scanning electron microscopy studies.

A scanning electron microscope (VEGA 3, TESCAN) examined the surfaces of the drug, physical mixture, and inclusion complexes. The sputter coater, Cressington 108, USA, coated the samples with a very thin coating of gold, which makes them conductive to electricity. Photos were collected at 20kV [42].

3. Results and Discussion

3.1. Phase solubility studies.

The diagram for the phase solubility of irbesartan with SBE7-β-CD and Me-β-CD is shown in Figure 2. The pure irbesartan solubility (s0) was 0.078 mg/ml. Over the entire concentration range studied, the solubility of irbesartan increases linearly with increasing modified β-cyclodextrin concentration, indicating an AL-type diagram. Therefore, inclusion complexes with an equal molar ratio (1:1) were prepared. The estimated Ks for irbesartan Me-β-CD inclusion complex was 584 ± 0.5 M-1 and for irbesartan SBE7-β-CD inclusion complex is 716 ± 0.69 M-1. Thus, it can be said that irbesartan makes more stable complexes with SBE7-β-CD. This may be because it makes the hydrophobic cavity bigger without steric hindrance and makes it easier to fit into the cavity [43,44].

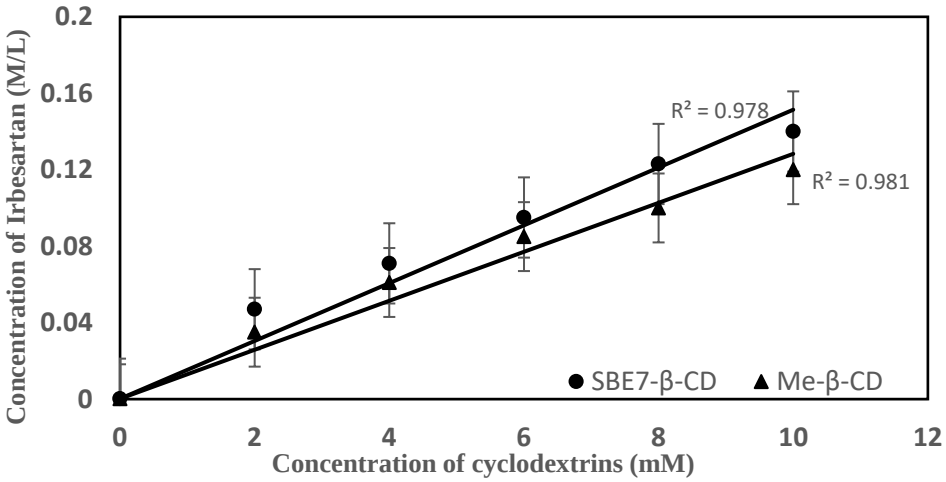

Figure 2. Phase solubility diagram of irbesartan with cyclodextrins.

3.2. Analysis of drug content.

Stat-Ease Design Expert 12 examined the cumulative effect of independent variables on response. The physical mixture and kneading inclusion complex of SBE$_7$-β-CD show a percentage drug content of 99.1±0.65, 98.25±0.85 respectively (n=3), whereas for Me-β-CD is 99.25±0.69 98.78±0.36. Nine batches of inclusion complexes of irbesartan with modified cyclodextrins were prepared, and the proportion of the medication present was determined. The findings are presented in Table 1.

Table 1. Experimental matrix of irbesartan inclusion complexes using 3^2 factorial design. (n=3)

Batch Number		Levels of independent variables employed		Irbesartan SBE7-β-CD Inclusion Complex	Irbesartan Me-β-CD Inclusion Complex
		X_1	X_2		
Std	Run	A: Power (W)	B: Time (Sec)	% Drug content	% Drug content
7	1	400	240	59.8 ± 0.23	58.9 ± 0.35
2	2	650	10	72.9 ± 0.56	75.7 ± 0.85
4	3	400	125	65.1 ± 0.78	68.9 ± 0.69
3	4	900	10	43.8 ± 1.52	41.7 ± 0.48
1	5	400	10	26.9 ± 0.98	30.8 ± 0.56
9	6	900	240	36.2 ± 0.17	35.6 ± 0.85
5	7	650	125	98.4 ± 0.28	99.2 ± 0.16
6	8	900	125	56.6 ± 0.96	55.8 ± 0.85
8	9	650	240	99.1 ± 0.26	95.5 ± 0.69

3.3. Preliminary trials.

The minimum power required for the reaction is 400 W for 10 seconds, and charring is observed at 500 seconds, whereas charring occurs at 250 seconds at 1000 W. The solvent quantity is kept constant in both conditions. The irradiated samples were stored in a desiccator and analyzed for drug content.

3.4. Experimental design and statistical data analysis.

The irbesartan inclusion complexes prepared with SBE$_7$-β-CD using microwave irradiation show percentage drug concentrations in the range of 26.9 ± 0.98 to 99.1 ± 0.26,

whereas with Me-β-CD is 30.8 ± 0.56 to 99.2 ± 0.16. The drug content in prepared inclusion complexes was significant ($p < 0.05$) in the quadratic model. Multiple linear regression generated polynomial model equations for all response variables. The polynomial equation relating the percentage drug content for irbesartan inclusion complexes prepared with SBE_7-β-CD using microwave irradiation is

$$R_1 = 101.41-2.53X_1+8.58X_2-10.13X_1X_2-42.07X_1^2-16.92X_2^2$$

The coefficient estimates provide the estimated response change per unit change in factor value, while all other factors are maintained constant. The adjusted R^2 of 0.9526 is close to the predicted R^2 of 0.8025. The difference is smaller than 0.2. Accuracy is employed as a measurement for the signal-to-noise ratio. The obtained value is 16.765. From the above model equation, F=33.18 indicates model significance. Terms in the model that have p-values less than 0.05 are considered significant. X_2, X_1X_2, X_{12}, and X_{22} significantly affect the percentage of drug content.

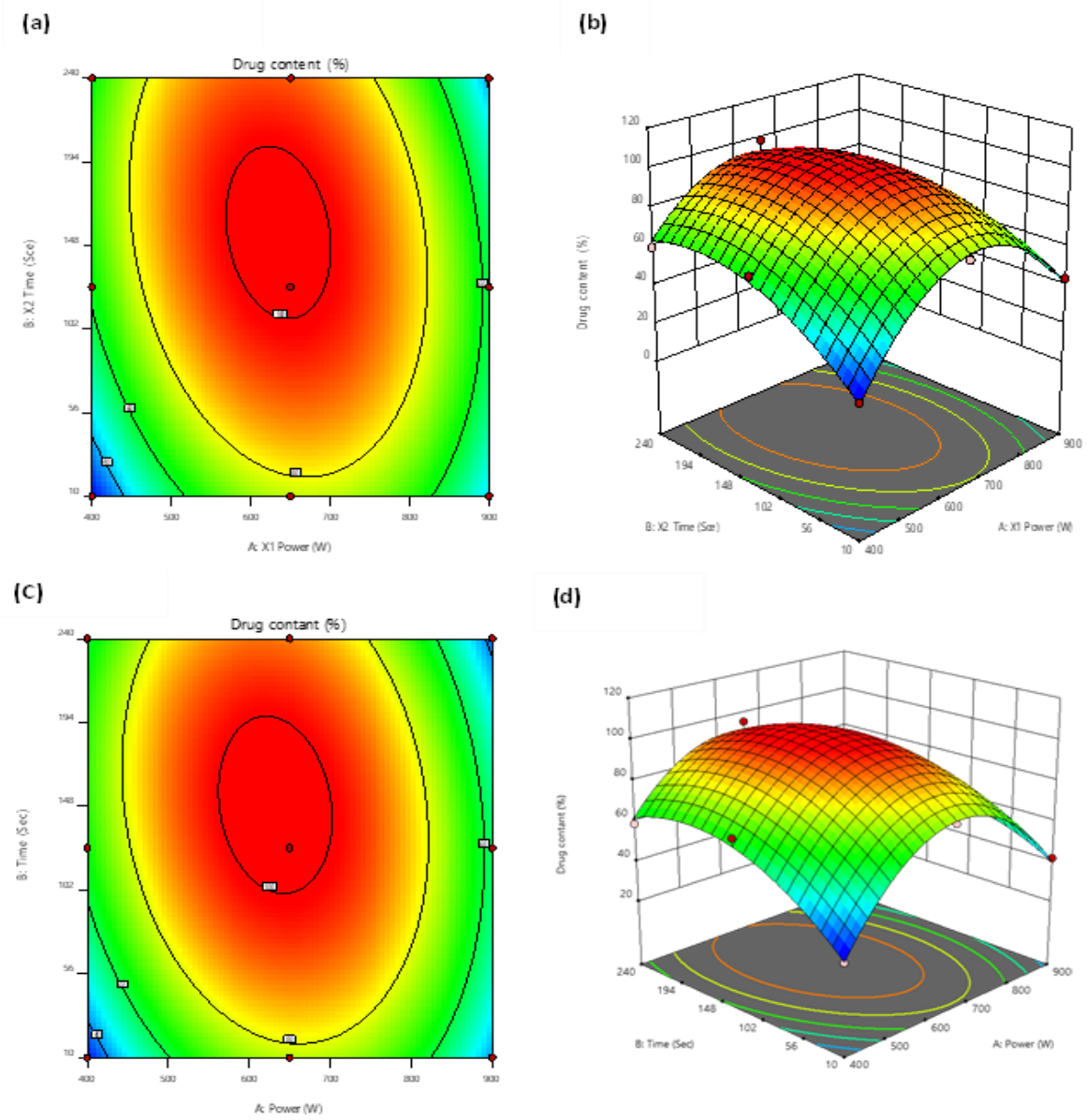

Figure 3. Two- dimensional contour plots and three-dimensional surface plots show the effects of process variables on percent drug content. **(a)** Irbesartan SBE_7-β-CD complex contour plot; **(b)** Irbesartan SBE_7-β-CD complex 3D surface plot; **(c)** Irbesartan Me-β-CD complex contour plot **(d)** Irbesartan Me-β-CD complex 3D surface plot.

The polynomial equation relating the percentage drug content for irbesartan inclusion complexes prepared with Me-β-CD using microwave irradiation is

$$R_2 = 102.31 - 4.25X_1 + 6.97X_2 - 8.55X_1X_2 - 41.52X_1^2 - 18.27X_2^2$$

The coefficient estimates provide the estimated response change per unit change in factor value, while all other factors are maintained constant. The discrepancy between the predicted R^2 value of 0.8624 and the adjusted R^2 value of 0.9653 is less than 0.2. Adequate precision determines the signal-to-noise ratio. The obtained value is 18.919. From the above model equation, F = 45.44 indicates model significance. Terms in the model that have P-values less than 0.05 are considered significant. X_2, X_1X_2, X_{12}, and X_{22} significantly affect the percentage of drug content.

A response surface approach was applied to learn more about how the combined effects of independent variables affect specified responses. Response surface methodology lets you plot response surfaces in three dimensions and contours in two dimensions. Three-dimensional response surface plots help explain the independent variables' main and interaction effects, whereas two-dimensional contour plots show the response values in Figure 3. The software made contour plots and 3D response plots that helped demonstrate how the data from the nine experimental runs on each response appeared. When power (X_1) and time (X_2) increase, drug content initially increases but then drops due to drug degradation at high power. The results also indicate an interaction between the variables, ultimately affecting the output.

3.5. Optimisation of process variables.

After constraining each component and response, the software suggested several independent variable ratios. Three inclusion ratios were chosen to test the model's optimization abilities. Numerical optimization was carried out by studying the desirability function; the target was within the range, and constraints were applied. The desirability function of selected solutions was found to be 1, indicating the model's suitability. After applying the constraints for the response presented in Figure 4, a graphical optimization was performed by building overlay graphs. The characteristics of these three batches indicated that the observed values of the batches were close to the values predicted by the software shown in Table 2. The observed percentage error ranges from -1.03 to 1.93, the lowest possible error rate, demonstrating that factorial models reliably predict process variables. The prepared inclusion complexes SMWC 3 and MMWC 3 were then tested and characterized for the dissolution rate.

Table 2. Optimization process variables for the preparation of inclusion complexes.

Responses	Batch	X1 Power(W)	X2 Time (Sec)	Observed Value (Mean± SD, n=3)	Predicted Value	% Error
Drug content in SBE7-β-CD irradiated inclusion complexes	SMWC 1	600	75	94.2± 0.45	92.42	1.93
	SMWC 2	600	85	95.8±0.78	95.04	0.80
	SMWC 3	600	97	96.5±0.36	96.59	-0.09
Drug content in Me-β-CD irradiated inclusion complexes	MMWC 1	600	71	92.6±0.32	93.56	-1.03
	MMWC 2	600	77	96.1±0.45	94.89	1.28
	MMWC 3	600	83	96.5±0.98	95.95	0.57

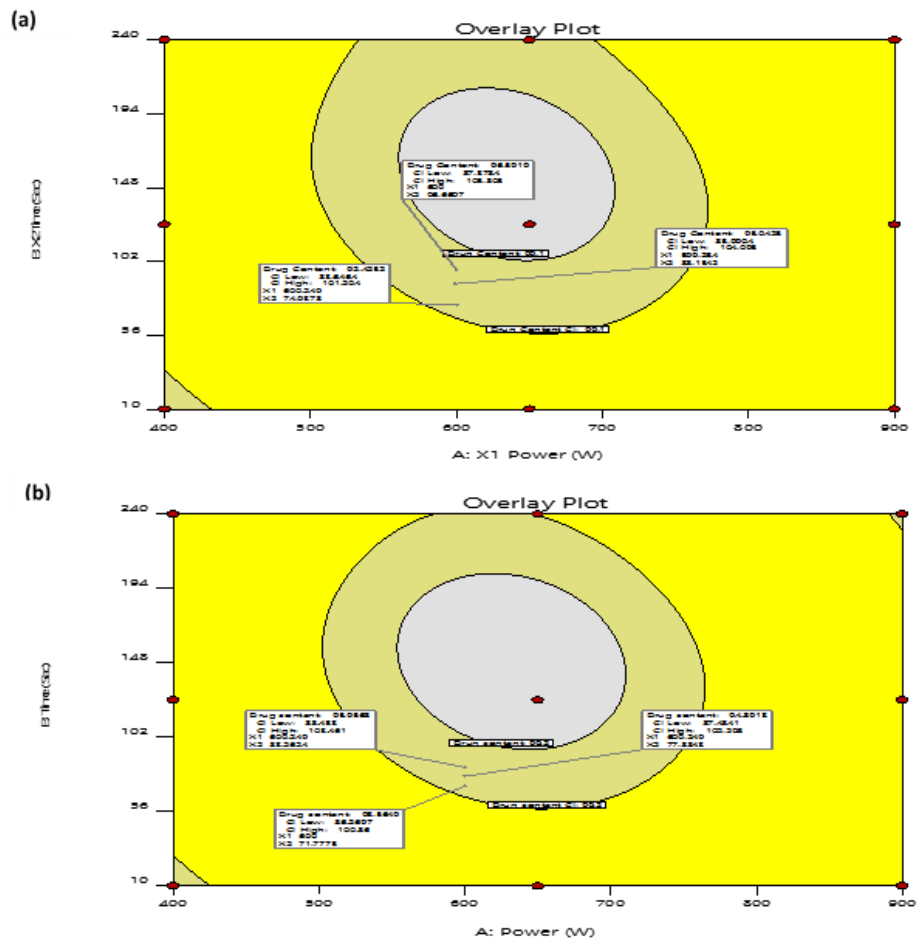

Figure 4. Graphical optimization by overlay plots indicating the region of optimal process variables. (**a**) Irbesartan SBE_7-β-CD microwave irradiation complexes; (**b**) Irbesartan SBE_7-β-CD microwave irradiation complexes.

3.6. Studies on in-vitro dissolution rate.

Pure drug and all inclusion complex dissolution curves are shown in Figure 5. These results showed that physical combination and kneading inclusion complex dissolved better than pure drug.

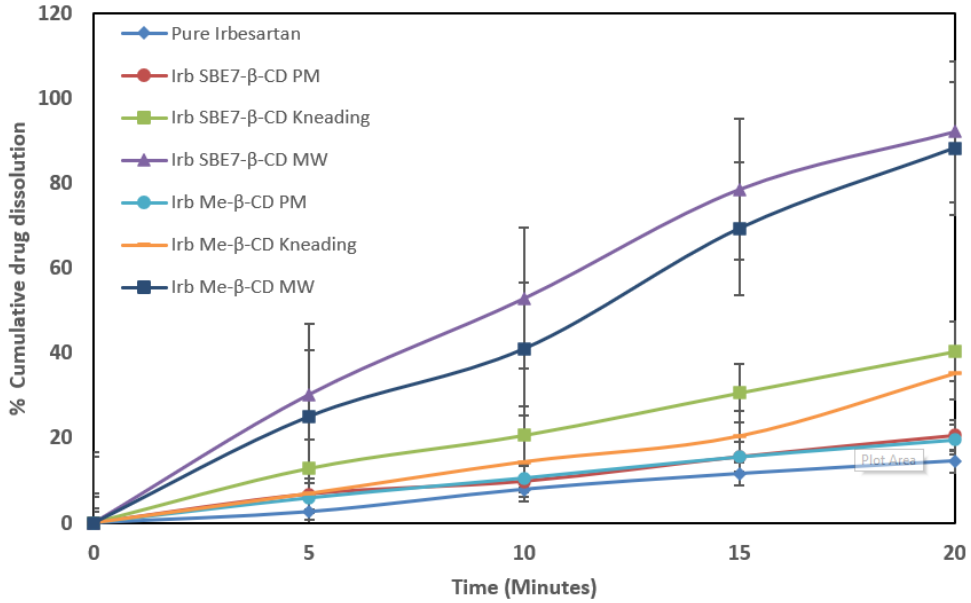

Figure 5. Dissolution profiles of irbesartan and irbesartan cyclodextrin complexes.

Irbesartan SBE_7-β-CD inclusion complex (SMWC 3) shows a higher rate of dissolution in comparison to that of the physical mixture and kneading inclusion complex. In the case of inclusion complexes prepared by the Me-β-CD, the inclusion complex (MMWC 3) showed a higher rate compared to the physical mixture and kneading complex. Microwave irradiation of inclusion complexes likely causes solubilization, amorphization, and enhanced wettability, all contributing to a higher dissolution rate. In both instances, the disintegration rate was enhanced in the ways described below: Irbesartan < physical mixture < kneading complex < microwave irradiated complex, suggesting that complex inclusion preparation affected dissolution. The microwave irradiation method enhances the dissolution rate of irbesartan by 6.31 folds by complexation with SBE_7-β-CD, whereas, in the case of Me-β-CD complexation, it is 6.04 folds.

3.7. Fourier transform infrared spectroscopy.

FTIR of irbesartan and complexes was recorded and is shown in Figure 6. FTIR spectrum of irbesartan shows the characteristic weak band at 3447 cm^{-1} related to N – H bond stretching vibration, steep apex at 2957 cm^{-1} related to C – H bond stretching of the aromatic ring, medium apex at 2871 cm^{-1} related to symmetric C – H bond stretching, very steep apex at 1730 cm^{-1} related to C = O bond stretching of carbonyl group, very steep apex at 1612 cm^{-1} related to N – H bond bending, medium intensity apex at 1483 cm^{-1} related to C = C bond stretching were observed which are similar to values reported in the literature [45]. The prepared inclusion complexes with SBE_7-β-CD showed a characteristic strong band at 3407 cm^{-1} related to N – H bond stretching vibration, steep apex at 2930 cm^{-1} related to C – H bond stretching of the aromatic ring, medium apex at 2851 cm^{-1} related to symmetric C – H bond stretching, steep apex at 1731 cm^{-1} related to C = O bond stretching of carbonyl group, steep apex at 1615 cm^{-1} related to N – H bond bending, medium intensity apex at 1433 cm^{-1} related to C = C bond stretching were observed. The prepared inclusion complexes with Me-β-CD showed characteristic strong bands at 3410 cm^{-1} related to N–H stretching vibration, a steep apex at 2925 cm^{-1} related to C–H bond stretching of an aromatic ring, a medium apex at 2834 cm^{-1} related to symmetric C–H bond stretching, a steep apex at 1731 cm^{-1} related to C = O bond stretching of the carbonyl group, a steep apex at 1615 cm^{-1} related to N–H bond bending, and a medium intensity apex at 1433 cm^{-1} related to C = C bond stretching were also observed. The decrease in peak intensity for C=O indicates the interaction with cyclodextrins.

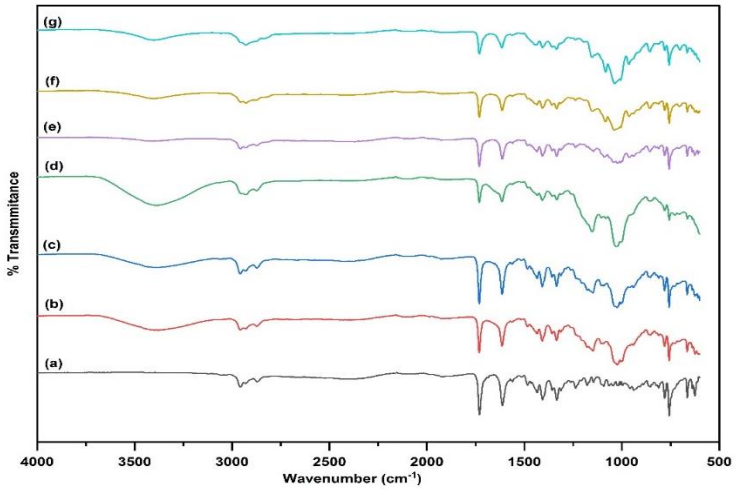

Figure 6. FTIR spectra of **(a)** Irbesartan; **(b)** Irbesartan SBE_7-β-CD PM; **(c)** Irbesartan SBE_7-β-CD PM Kneading complex; **(d)** Irbesartan SBE_7-β-CD MW; **(e)** Irbesartan Me-β-CD PM; **(f)** Irbesartan Me-β-CD Kneading; **(g)** Irbesartan Me-β-CD MW.

3.8. Thermal analysis.

The differential scanning calorimetric curve of irbesartan and inclusion complexes, shown in Figure 7, gave information about the solid-state interactions and the influence of preparation methods. Irbesartan differential scanning calorimetry data revealed an endothermic peak relatively sharp at 186 °C, resembling the value reported in the literature [46]. After that, there is an immediate release of heat and a mass loss due to decomposition at 212 °C, which ends at 273 °C with a peak at 244 °C. SBE7-β-CD showed an endothermic peak at 275°C [47,48]. The physical mixture of irbesartan and SBE7-β-CD shows both the peaks representing the drug and SBE7-β-CD. In the kneading thermogram, the irbesartan and SBE7-β-CD peaks had decreased intensities, with a broad peak at 275 °C, implying little interaction between irbesartan and SBE7-β-CD. Irbesartan SBE7-β-CD microwave irradiated complex peaked at 180 °C, indicating the formation of an inclusion complex. The thermogram of methyl-β-cyclodextrin showed a broad endothermic peak starting from 45° C to 111°C associated with water loss. The physical mixture of irbesartan and Me-β-CD shows both the peaks representing the drug and Me-β-CD. The kneading complex thermogram of irbesartan and Me-β-CD showed a broad peak at 170 °C, indicating interaction and complex formation. A broad peak at 173.1 °C was observed in the microwave-irradiated complex of irbesartan Me-β-CD, indicating complex formation.

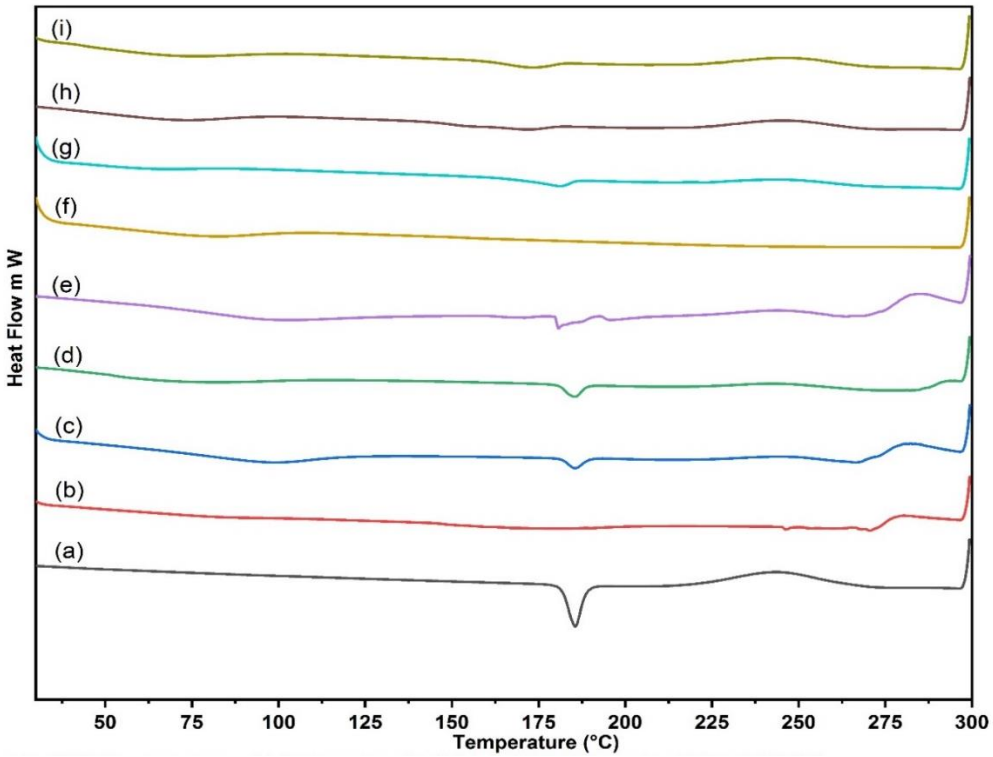

Figure 7. DSC thermogram of **(a)** Irbesartan; **(b)** SBE_7-β-CD; **(c)** Irbesartan SBE_7-β-CD PM; **(d)** Irbesartan SBE_7-β -CD Kneading complex; **(e)** Irbesartan SBE_7-β-CD MW complex; **(f)** Me -β-CD; **(g)** Irbesartan Me-β-CD PM; **(h)** Irbesartan Me-β-CD Kneading complex; **(i)** Irbesartan Me-β-CD MW complex.

3.8. Powder X-ray diffraction.

The crystalline nature of irbesartan in complexes was investigated with X-ray diffraction studies shown in Figure 8. The irbesartan showed crystalline sharp peaks at 10.38°, 12.24°, 13.18°, 16.82°, 17.65°, 18.87°, 19.4°, 19.96°, 20.64°, 21.19°, 21.46°, 22.55°, 22.95°, 23.49°, 26.58°, 27.41°, 28.39°, 31.84°, 32.95°, 37.12°, and 41.68° (2θ) [49]. SBE_7-β-CD shows

a diffraction pattern indicative of an amorphous nature. The physical mixture of irbesartan SBE7-β-CD shows a similar diffraction pattern as that of pure irbesartan with slight variation in intensity. The SBE7-β-CD kneading complex showed peaks at 10.84°, 12.54°, 13.39°, 15.6°, 16.2°, 17.18°, 19.55°, 20.10°, 21.90°, 23.5°, 27.67°, 28.8°, 32.2°, 37.55°, and 39.9°. The microwave irradiation complex of SBE7-β-CD peaks at 10.96°, 12.64°, 13.42°, 14.33°, 15.88°, 17.16°, 18.89°, 19.61°, 20.40°, 21.69°, 23.24°, 25.56°, 28.0°, 29.31°, and 31.2°. Me-β-CD showed a diffraction pattern indicative of an amorphous nature. The physical mixture of irbesartan Me-β-CD shows a similar diffraction pattern as that of pure irbesartan with slight variation in intensity. The Me-β-CD kneading complex showed peaks at 10.64°, 12.54°, 13.1°, 17.1°,18.9°,19.5°, 20.5°, 21.52°, 22.8°, 23.3°, 26.6°, 27.9° and 33.33°. The microwave irradiation complex of Me-β-CD peaks at 10.55°, 11.61°, 12.31°, 12.54°, 13.35°, 14.71°, 16.61°, 17.08°, 17.61°, 19.07°, 19.53°, 20.0°, 20.8°, 21.76°, 23.27°, 24.79°, 26.78°, 27.71°, 28.64°, and 32.02°. The irbesartan degree of crystallinity was found to be 63.80 percent. The irbesartan SBE7-β-CD microwave irradiated complex was 48.52 percent, while the complex of irbesartan Me-β-CD was 61.90 percent.

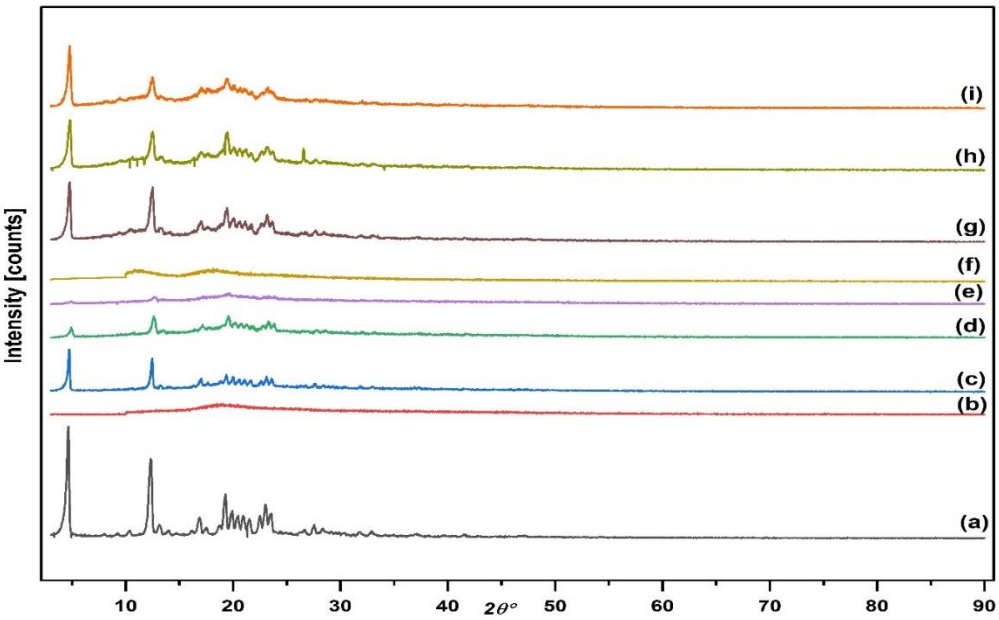

Figure 8. XRD plots of **(a)** Irbesartan; **(b)** SBE7-β-CD; **(c)** Irbesartan SBE7-β-CD PM; **(d)** Irbesartan SBE7-β-CD kneading; **(e)** Irbesartan SBE7-β-CD; **(f)** Methyl-β-CD; **(g)** Irbesartan Me-β-CD PM; **(h)** Irbesartan Me-β-CD kneading; **(i)** Irbesartan Me-β-CD MW.

3.9. Scanning electron microscopy (SEM) studies.

The morphology and particle size of irbesartan, kneading complexes, and microwave-irradiated complexes were analyzed by SEM and shown in Figure 9. Irbesartan appeared as rod-shaped crystals [50]. In the physical mixture of irbesartan SBE7-β-CD, it is observed that irbesartan crystals combined and attached to SBE7-β-CD particles, showing no solid-state interaction. The kneading complex for irbesartan SBE7-β-CD showed slight interaction between them. The irbesartan SBE7-β-CD microwave irradiated complex showed large, irregular-shaped particles, indicating the formation of particles of an amorphous nature. Following the inclusion complex with Me-β-CD, particles lost form, smoothed, and shrank. Inclusion complexes changed drug particle morphology and shaped drastically. Irbesartan and Me-β-CD were indistinguishable, suggesting a high degree of complexation.

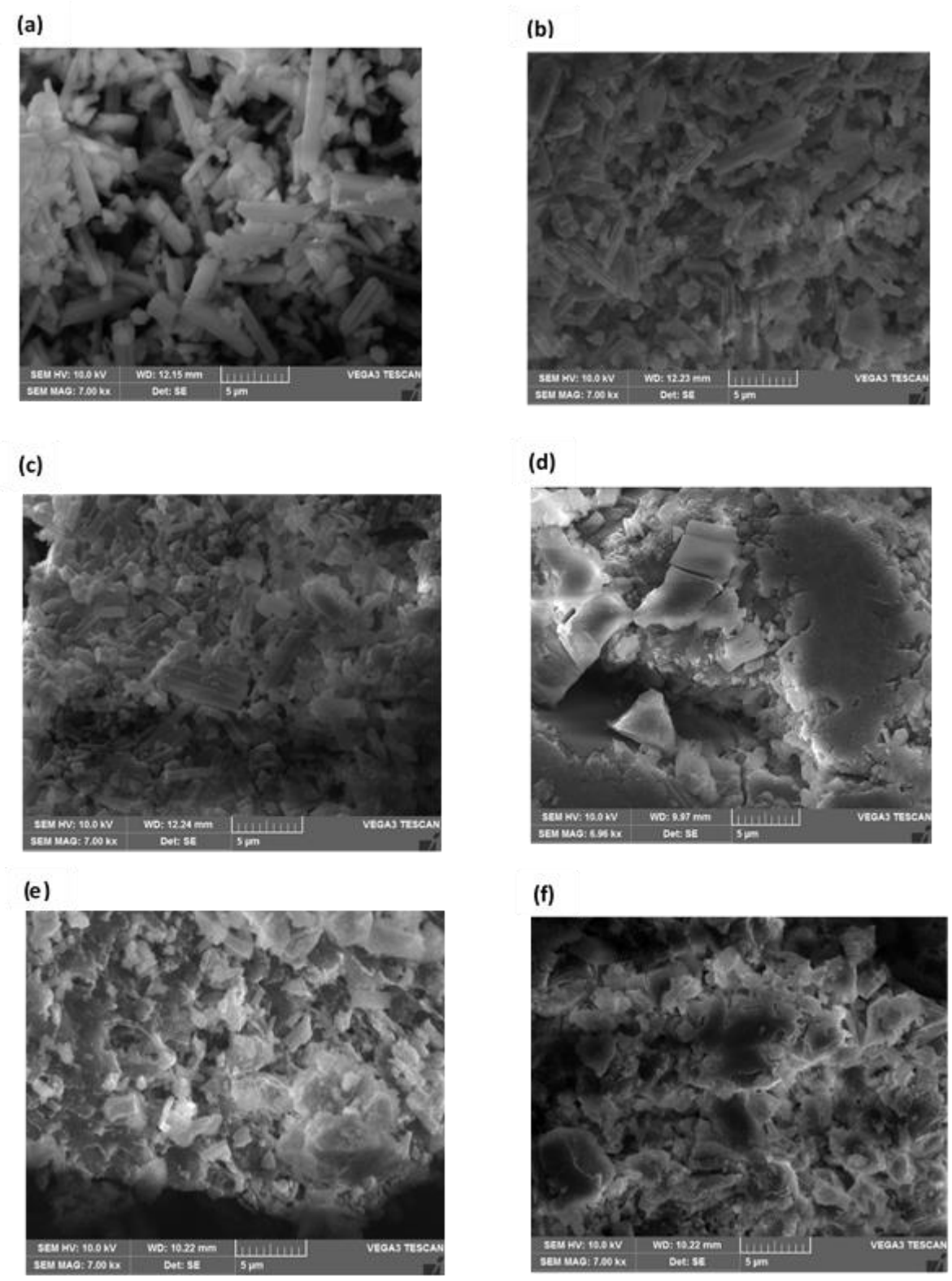

Figure 9. SEM images of **(a)** Irbesartan; **(b)** Irbesartan SBE_7-β-CD PM; **(c)** Irbesartan SBE_7-β-CD Kneading complex; **(d)** Irbesartan SBE_7-β-CD MW complex; **(e)** Irbesartan Me-β-CD Kneading complex; **(f)** Irbesartan Me-β-CD MW complex.

4. Conclusions

In this study, adding modified cyclodextrins made irbesartan more soluble because of electronic interactions. The phase solubility experiments reveal AL-type curves; hence, inclusion complexes were prepared using an equal molar ratio. Irbesartan inclusion complexes

were produced using the kneading and microwave irradiation techniques with SBE7-β-CD and Me-β-CD. The process variables in the microwave irradiation technique for preparing irbesartan and modified β-cyclodextrin inclusion complexes were optimized using a 32-factorial design. The prepared inclusion complexes SMWC 3 and MMWC 3 were further used for dissolution rate testing and characterization. The irbesartan inclusion complexes with SBE7-β-CD prepared by kneading technique showed 2.76 folds. The microwave irradiation technique (SMWC 3) showed 6.31 folds enhanced dissolution rate compared with pure irbesartan, where the Me-β-CD complexes showed 2.14 and 6.04 folds, respectively. The DSC thermographs of microwave-irradiated complexes indicated solid-state interaction, and X-ray diffraction revealed the amorphization of irbesartan in the complexes. The FTIR spectra indicate no significant change in the characteristic peaks of functional groups. The SEM images for SMWC 3 and MMWC 3 revealed drastic changes in the structure of the inclusion complexes, namely the morphology and form of the drug particles. Thus, this combination improves irbesartan oral bioavailability at an appropriate dosage form.

Funding

This research received no external funding.

Acknowledgments

The author acknowledges the assistance of the CoExAMMPC at Vignan's Foundation for Science, Technology, & Research in characterizing the samples and Krishna University for providing a laboratory facility.

Conflicts of Interest

The authors declare no conflict of interest.

References

1. Irbesartan. In *Drugs and Lactation Database (LactMed)*; Bethesda (MD), **2006**.
2. Malishevskii, M.V. [Irbesartan in clinical practice]. *Kardiologiia* **2012**, *52*, 66-74, https://pubmed.ncbi.nlm.nih.gov/23237398/.
3. Meruva, S.; Thool, P.; Shah, S.; Karki, S.; Bowen, W.; Ghosh, I.; Kumar, S. Formulation and performance of Irbesartan nanocrystalline suspension and granulated or bead-layered dried powders - Part I. *Int J Pharm* **2019**, *568*, 118189, https://doi.org/10.1016/j.ijpharm.2019.03.007.
4. Darwish, I.A.; Darwish, H.W.; Bakheit, A.H.; Al-Kahtani, H.M.; Alanazi, Z. Irbesartan (a comprehensive profile). *Profiles Drug Subst Excip Relat Methodol* **2021**, *46*, 185-272, https://doi.org/10.1016/bs.podrm.2020.07.004.
5. Chawla, G.; Bansal, A.K. A comparative assessment of solubility advantage from glassy and crystalline forms of a water-insoluble drug. *Eur J Pharm Sci* **2007**, *32*, 45-57, https://doi.org/10.1016/j.ejps.2007.05.111.
6. Akram, A.; Irfan, M.; Abualsunun, W.A.; Bukhary, D.M.; Alissa, M. How to Improve Solubility and Dissolution of Irbesartan by Fabricating Ternary Solid Dispersions: Optimization and In-Vitro Characterization. *Pharmaceutics* **2022**, *14*, https://doi.org/10.3390/pharmaceutics14112264.
7. Soe, H.; Sripetch, S.; Loftsson, T.; Stefansson, E.; Jansook, P. Effect of Soluplus((R)) on gamma-cyclodextrin solubilization of irbesartan and candesartan and their nanoaggregates formation. *Pharm Dev Technol* **2022**, *27*, 9-18, https://doi.org/10.1080/10837450.2021.2017968.
8. Challa R, A.A., Ali J, Khar RK. Cyclodextrins in Drug Delivery: An Updated Review. *AAPS PharmSciTech* **2005**, *06*, https://doi.org/10.1208/pt060243.
9. Davis, M.E.; Brewster, M.E. Cyclodextrin-based pharmaceutics: past, present and future. *Nat Rev Drug Discov* **2004**, *3*, 1023-1035, https://doi.org/10.1038/nrd1576.

10. Liu, M.; Zheng, C.; Zheng, Y.; Wu, X.; Shen, J. Binding model-tuned room-temperature phosphorescence of the bromo-naphthol derivatives based on cyclodextrins. *RSC Adv* **2022**, *12*, 19313-19316, https://doi.org/10.1039/d2ra03046b.
11. Kim, H.C.; Kwon, Y.R.; Kim, J.S.; Kwon, M.; Kim, J.H.; Kim, D.H. Computational Approach to the Surface-Crosslinking Process of Superabsorbent Polymer via Central Composite Design. *Polymers (Basel)* **2022**, *14*, 3842, https://doi.org/10.3390/polym14183842.
12. Zhou, J.; Jia, J.; He, J.; Li, J.; Cai, J. Cyclodextrin Inclusion Complexes and Their Application in Food Safety Analysis: Recent Developments and Future Prospects. *Foods* **2022**, *11*, 3871, https://doi.org/10.3390/foods11233871.
13. Sakai, K.; Sato, Y.; Okada, M.; Yamaguchi, S. Cyclodextrins produced by cyclodextrin glucanotransferase mask beany off-flavors in plant-based meat analogs. *PLoS One* **2022**, *17*, https://doi.org/10.1371/journal.pone.0269278.
14. Hirlekar, R.; Kadam, V. Preformulation study of the inclusion complex irbesartan-beta-cyclodextrin. *AAPS PharmSciTech* **2009**, *10*, 276-281, https://doi.org/10.1208/s12249-009-9206-5.
15. Leonis, G.; Christodoulou, E.; Ntountaniotis, D.; Chatziathanasiadou, M.V.; Mavromoustakos, T.; Naziris, N.; Chountoulesi, M.; Demetzos, C.; Valsami, G.; Damalas, D.E.; et al. Antihypertensive activity and molecular interactions of irbesartan in complex with 2-hydroxypropyl-beta-cyclodextrin. *Chem Biol Drug Des* **2020**, *96*, 668-683, https://doi.org/10.1111/cbdd.13664.
16. Fang, S.; Peng, X.; Liang, X.; Shen, J.; Wang, J.; Chen, J.; Meng, Y. Enhancing Water Solubility and Stability of Natamycin by Molecular Encapsulation in Methyl-β-Cyclodextrin and its Mechanisms by Molecular Dynamics Simulations. *Food Biophysics* **2019**, *15*, 188-195, https://doi.org/10.1007/s11483-019-09620-z.
17. Fukuda, M.; Miller, D.A.; Peppas, N.A.; McGinity, J.W. Influence of sulfobutyl ether beta-cyclodextrin (Captisol) on the dissolution properties of a poorly soluble drug from extrudates prepared by hot-melt extrusion. *Int J Pharm* **2008**, *350*, 188-196, https://doi.org/10.1016/j.ijpharm.2007.08.038.
18. Vicatos, A.I.; Hoossen, Z.; Caira, M.R. Inclusion complexes of the steroid hormones 17beta-estradiol and progesterone with beta- and gamma-cyclodextrin hosts: syntheses, X-ray structures, thermal analyses and API solubility enhancements. *Beilstein J Org Chem* **2022**, *18*, 1749-1762, https://doi.org/10.3762/bjoc.18.184.
19. Nagai, N.; Ogata, F.; Ike, A.; Shimomae, Y.; Osako, H.; Nakazawa, Y.; Yamamoto, N.; Kawasaki, N. Oral Formulation Based on Irbesartan Nanocrystals Improve Drug Solubility, Absorbability, and Efficacy. *Pharmaceutics* **2022**, *14*, 387, https://doi.org/10.3390/pharmaceutics14020387.
20. Yan, V.C.; Muller, F.L. Captisol and GS-704277, but Not GS-441524, Are Credible Mediators of Remdesivir's Nephrotoxicity. *Antimicrob Agents Chemother* **2020**, *64*, https://doi.org/10.1128/AAC.01920-20.
21. Yurtdas-Kirimlioglu, G. Spray dried nanospheres for inclusion complexes of cefpodoxime proxetil with beta-cyclodextrin, 2-hydroxypropyl-beta-cyclodextrin and methyl-beta-cyclodextrin: improved dissolution and enhanced antibacterial activity. *Drug Dev Ind Pharm* **2021**, *47*, 1261-1278, https://doi.org/10.1080/03639045.2021.1989452.
22. Hedges, A.R. Industrial Applications of Cyclodextrins. *Chem. Rev* **1998**, *98*, 2035−2044, https://doi.org/10.1021/cr970014w.
23. Ramos-Martinez, B.; Davila-Pousa, C.; Merino-Bohorquez, V.; Garcia-Palomo, M.; Flox-Benitez, M.f. Use of cyclodextrins as excipients in pharmaceutical products: why not in extemporaneous preparations? *Farm Hosp* **2021**, *46*, 31-39, https://pubmed.ncbi.nlm.nih.gov/35379090/.
24. Nacsa, A.; Ambrus, R.; Berkesi, O.; Szabo-Revesz, P.; Aigner, Z. Water-soluble loratadine inclusion complex: analytical control of the preparation by microwave irradiation. *J Pharm Biomed Anal* **2008**, *48*, 1020-1023, https://doi.org/10.1016/j.jpba.2008.07.001.
25. Mohit, V.; Harshal, G.; Neha, D.; Vilasrao, K.; Rajashree, H. A comparative study of complexation methods for cefdinir-hydroxypropyl-β-cyclodextrin system. *Journal of Inclusion Phenomena and Macrocyclic Chemistry* **2010**, *71*, 57-66, https://doi.org/10.1007/s10847-010-9901-6.
26. Kaushal, S.; Singh, I.; Singh, S.; Gupta, A. Sustainable advanced manufacturing and materials processing : methods and technologies. **2023**, 1. Available online: https://www.routledge.com/Sustainable-Advanced-Manufacturing-and-Materials-Processing-Methods-and/Kaushal-Singh-Singh-Gupta/p/book/9781032216263.

27. Mageswari, K.; Prabukanthan, P.; Madhavan, J. Microwave-assisted synthesis of ZnO nanoparticles using different capping agents and their photocatalytic application. *Environ Sci Pollut Res Int* **2023**, https://doi.org/10.1007/s11356-022-25097-9.
28. Xu, W.J.; Xie, H.J.; Cao, Q.R.; Shi, L.L.; Cao, Y.; Zhu, X.Y.; Cui, J.H. Enhanced dissolution and oral bioavailability of valsartan solid dispersions prepared by a freeze-drying technique using hydrophilic polymers. *Drug Deliv* **2016**, *23*, 41-48, https://doi.org/10.3109/10717544.2014.903012.
29. Higuchi, T., Connors, K.A. Phase solubility techniques. *Advances in Analytical Chemistry and Instrumentation* **1965**, *4*, 117, https://www.scienceopen.com/document?vid=76f1d8c7-413c-40f2-aa7f-227482d5d1ad.
30. Ranpise, N.S.; Kulkarni, N.S.; Mair, P.D.; Ranade, A.N. Improvement of water solubility and in vitro dissolution rate of aceclofenac by complexation with beta-cyclodextrin and hydroxypropyl-beta-cyclodextrin. *Pharm Dev Technol* **2010**, *15*, 64-70, https://doi.org/10.3109/10837450903002165.
31. Ghosh, A.; Biswas, S.; Ghosh, T. Preparation and Evaluation of Silymarin beta-cyclodextrin Molecular Inclusion Complexes. *J Young Pharm* **2011**, *3*, 205-210, https://doi.org/10.4103/0975-1483.83759.
32. Cirri, M.; Maestrelli, F.; Mennini, N.; Mura, P. Physical-chemical characterization of binary and ternary systems of ketoprofen with cyclodextrins and phospholipids. *J Pharm Biomed Anal* **2009**, *50*, 683-689, https://doi.org/10.1016/j.jpba.2008.11.003.
33. Moneghini, M.; Bellich, B.; Baxa, P.; Princivalle, F. Microwave generated solid dispersions containing Ibuprofen. *Int J Pharm* **2008**, *361*, 125-130, https://doi.org/10.1016/j.ijpharm.2008.05.026.
34. Das, S.; Mohanty, S.; Maharana, J.; Jena, S.R.; Nayak, J.; Subuddhi, U. Microwave-assisted β-cyclodextrin/chrysin inclusion complexation: An economical and green strategy for enhanced hemocompatibility and chemosensitivity in vitro. *Journal of Molecular Liquids* **2020**, *310*, https://doi.org/10.1016/j.molliq.2020.113257.
35. Remón, J.; Zhu, G.; Budarin, V.L.; Clark, J.H. Analysis and optimisation of a microwave-assisted hydrothermal process for the production of value-added chemicals from glycerol. *Green Chemistry* **2018**, *20*, 2624-2636, https://doi.org/10.1039/c8gc01079j.
36. Godbole, M.D.; Sabale, P.M.; Mathur, V.B. Development of lamivudine liposomes by three-level factorial design approach for optimum entrapment and enhancing tissue targeting. *J Microencapsul* **2020**, *37*, 431-444, https://doi.org/10.1080/02652048.2020.1778806.
37. Ahmad, N.; Ahmad, R.; Al-Qudaihi, A.; Alaseel, S.E.; Fita, I.Z.; Khalid, M.S.; Pottoo, F.H. Preparation of a novel curcumin nanoemulsion by ultrasonication and its comparative effects in wound healing and the treatment of inflammation. *RSC Adv* **2019**, *9*, 20192-20206, https://doi.org/10.1039/c9ra03102b.
38. The United States pharmacopeia. The National formulary. **2010**. Available online: https://az.research.umich.edu/animalcare/informational/united-states-pharmacopeia-national-formulary-usp-nf.
39. Smith, B. *Infrared Spectral Interpretation: A Systematic Approach*; CRC Press: **2018**.
40. Yihong Qiu, Y.C., Geoff G.Z. Zhang, Lawrence Yu, Rao V. Mantri. *Developing Solid Oral Dosage Forms_ Pharmaceutical Theory and Practice*; Academic Press **2016**, https://www.elsevier.com/books/developing-solid-oral-dosage-forms/qiu/978-0-12-802447-8.
41. Bunaciu, A.A.; Udristioiu, E.G.; Aboul-Enein, H.Y. X-ray diffraction: instrumentation and applications. *Crit Rev Anal Chem* **2015**, *45*, 289-299, https://doi.org/10.1080/10408347.2014.949616.
42. Ni, C. Scanning Electron Microscopy (SEM). In *Encyclopedia of Tribology*, Wang, Q.J., Chung, Y.-W., Eds.; Springer US: Boston, MA, **2013**, 2977-2982, https://link.springer.com/referenceworkentry/10.1007/978-0-387-92897-5_1217.
43. Lankapalli, S.; Suryadevara, V.; Sunkara, S.; Sakhamuri, V.; Danda, H. Dissolution rate enhancement of irbesartan and development of fast-dissolving tablets. *Egyptian Pharmaceutical Journal* **2016**, *15*, https://doi.org/10.4103/1687-4315.197583.
44. Yousef, F. Effect of pH on the complexation of irbesartan with hydroxypropyl-β, and γ-cyclodextrin: solubility enhancement and physicochemical characterization. *Turkish Journal of Chemistry* **2018**, *42*, 1544-1558, https://doi.org/10.3906/kim-1805-22.
45. Franca, C.A.; Etcheverry, S.B.; Pis Diez, R.; Williams, P.A.M. Irbesartan: FTIR and Raman spectra. Density functional study on vibrational and NMR spectra. *Journal of Raman Spectroscopy* **2009**, *40*, 1296-1300, https://doi.org/10.1002/jrs.2282.

46. Skotnicki, M.; Jadach, B.; Skotnicka, A.; Milanowski, B.; Tajber, L.; Pyda, M.; Kujawski, J. Physicochemical Characterization of a Co-Amorphous Atorvastatin-Irbesartan System with a Potential Application in Fixed-Dose Combination Therapy. *Pharmaceutics* **2021**, *13*, https://doi.org/10.3390/pharmaceutics13010118.
47. Beig, A.; Agbaria, R.; Dahan, A. The use of captisol (SBE7-beta-CD) in oral solubility-enabling formulations: Comparison to HPbetaCD and the solubility-permeability interplay. *Eur J Pharm Sci* **2015**, *77*, 73-78, https://doi.org/10.1016/j.ejps.2015.05.024.
48. Gatiatulin, A.K.; Grishin, I.A.; Buzyurov, A.V.; Mukhametzyanov, T.A.; Ziganshin, M.A.; Gorbatchuk, V.V. Determination of Melting Parameters of Cyclodextrins Using Fast Scanning Calorimetry. *Int J Mol Sci* **2022**, *23*, https://doi.org/10.3390/ijms232113120.
49. Araya-Sibaja, A.M.; Fandaruff, C.; Guevara-Camargo, A.M.; Vargas-Huertas, F.; Zamora, W.J.; Vega-Baudrit, J.R.; Guillen-Giron, T.; Navarro-Hoyos, M.; Paoli, P.; Rossi, P.; et al. Crystal Forms of the Antihypertensive Drug Irbesartan: A Crystallographic, Spectroscopic, and Hirshfeld Surface Analysis Investigation. *ACS Omega* **2022**, *7*, 14897-14909, https://doi.org/10.1021/acsomega.2c00545.
50. Tian, J.; Ting Meng, T.; Ma, S.; Gao, T.; Di, X.; Chen, J.; Yang, J. Spatial-thermodynamic understanding of stabilization mechanism using computational approaches and molecular-level elucidation of the mechanism of crystal transformation in polymorphic irbesartan nanosuspensions. *Int J Pharm* **2022**, *612*, 121350, https://doi.org/10.1016/j.ijpharm.2021.121350.